ChemComm

Valence tautomerism in a [2×2] Co4 grid complex containing a ditopic arylazo ligand

Journal:	*ChemComm*
Manuscript ID	CC-COM-04-2021-001991.R2
Article Type:	Communication

COMMUNICATION

Valence tautomerism in a [2×2] Co_4 grid complex containing a ditopic arylazo ligand

Received 00th January 20xx,
Accepted 00th January 20xx

DOI: 10.1039/x0xx00000x

Nico M. Bonanno,[a] Zackery Watts,[a] Cole Mauws,[b] Brian O. Patrick,[d] Christopher R. Wiebe,[b,c] Yuki Shibano,[e] Kenji Sugisaki,[e*] Hideto Matsuoka,[e] Daisuke Shiomi,[e] Kazunobu Sato,[e*] Takeji Takui,[e*] and Martin T. Lemaire[a*]

We describe the structural and magnetic properties of a tetranuclear [2×2] Co_4 grid complex containing a ditopic arylazo ligand. At low temperatures and in solution the complex is comprised of Co^{3+} and singly reduced trianion-radical ligands. In the solid state we demonstrate the presence of valence tautomerization via variable temperature magnetic susceptibility experiments and powder-pattern EPR spectroscopy. Valence tautomerism in polynuclear complexes is very rare and to our knowledge is unprecedented in [2×2] grid complexes.

Molecular switching can take many forms, including photo-switching, guest-dependent binding, and mechanically interlocked systems, which are of interest as "molecular motors".[1,2] One of the best examples of molecular switching can occur in six-coordinate transition metal complexes with d^4-d^7 configurations in the form of spin-crossover.[3,4] Spin-crossover complexes exhibit an equilibrium between high- and low-spin states that can be tipped in either direction through application of an external stimulus. Strong cooperative interactions in molecular spin-crossover complexes can give rise to abrupt spin transitions, thermal hysteresis and bistability.[5–9]

Valence tautomerism (VT) is another form of paramagnetic switching but that relies upon the coordination of redox-active ligands to transition metal ions (later first row transition metals like Fe, Co, Ni, Cu; however, VT has also been reported for Ru and Yb complexes).[10,11] The prototypical valence tautomer family includes cobalt-dioxolene complexes of the general form (LL)Co(diox)$_2$ (where LL = bidentate ancillary ligand).[12] In these complexes, both spin-crossover at cobalt and electron transfer between cobalt and a coordinated dioxolene occur in response to a change in temperature.[13] Like spin-crossover complexes, valence tautomeric transitions can be abrupt with hysteresis when there are strong cooperative interactions.[14,15] Reported VT complexes are far fewer than their spin-crossover counterparts, owing to the difficulty generating ligand systems capable of reversible electron transfer reactions. Non-dioxolene containing VT complexes are rare but VT has been observed in transition metal complexes with other redox active ligands, notably iminosemiquione and salen-type ligands, but also recently in some others, including verdazyl and nitronyl nitroxide radicals.[16–31] VT in copper complexes containing 2,3,5,6-*tetrakis*-(tetramethylguanidino)pyridine ligand has also recently been reported.[32] Most reported VT complexes are mononuclear but recent efforts have led to a number of new binuclear VT complexes by following one of two synthetic strategies: (1) Coordinating Co(diox)$_2$ units to bridging N-donor ditopic chelating ligands or (2) coordination of bridging dioxolene ligands to cobalt bound to a tetradentate ancillary ligand.[33–42] VT complexes with nuclearity beyond two are very rare.[43] Recently, Li *et al.* reported a trinuclear cobalt VT complex "triangle" also containing tetrazine-based bridging radical anions and investigated the VT mechanism in detail using density functional theory (DFT).[44] Another class of redox-active ligand with an extensive coordination chemistry is the arylazo family.[45,46] Open-shell ligand oxidation states have been identified in arylazo complexes but the observation of thermally reversible electron transfer between a transition metal and a coordinated arylazo ligand has not been demonstrated to our knowledge.[47–49] Herein, we describe the preparation of a new ditopic arylazo ligand (H_2L^1, Figure 1), which produces a neutral $Co_4L^1_4$ [2×2] grid complex (**1**) that is shown to undergo VT in the solid state.

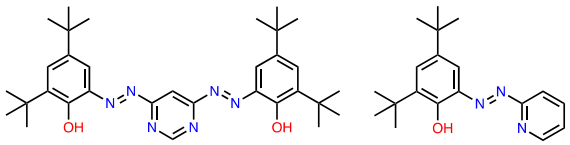

[a]*Department of Chemistry, Brock University, St. Catharines, ON, L2S 3A1.*
[b]*Department of Chemistry, University of Manitoba, Winnipeg, MB, R3T 2N2.*
[c]*Department of Chemistry, University of Winnipeg, Winnipeg, MB, R3B 2E9.*
[d]*Department of Chemistry, University of British of Columbia, Vancouver, BC, V6T 1Z1.*
[e]*Department of Chemistry and Molecular Materials Science, Graduate School of Science, Osaka City University, Osaka 558 8585, Japan.*
Electronic Supplementary Information (ESI) available: The Supporting Information includes synthetic details, spectroscopic, electrochemical, computational and single crystal X-ray data (PDF). Crystallographic data for CCDC 1922364 (CIF). Crystallographic data for CCDC 1922365 (CIF). See DOI: 10.1039/x0xx00000x

Figure 1. Structures of ditopic H_2L^1 (left) and monotopic HL^2 (right) ligands.

The ligand H_2L^1 was prepared in two steps, first by reaction of 4,6-dichloro-1,3-pyrimidine with hydrazine to produce the *bis*(hydrazide) followed by reaction with 3,5-di-*tert*-butyl-1,2-benzoquinone to generate H_2L^1 as the enol tautomer (ESI†), which was spectroscopically confirmed (ESI†). Combination of H_2L^1 with $Co(ClO_4)_2{\cdot}6H_2O$ in methanol produced a dark precipitate and was recrystallized from acetonitrile/DCM to generate single crystals suitable for X-ray diffraction. Data was collected at 100(2) K and the structure was solved and refined as a 4-component inversion twin (Figure 2). In the crystal structure there are two quarter molecules of complex **1** in the asymmetric unit. There are no perchlorate anions in the structure. Disordered solvent was identified in the asymmetric unit but could not be adequately modeled and was removed using the SQUEEZE routine. Co-crystallized solvent in **1** was calculated based on elemental analysis and thermogravimetric analysis (ESI†) results. In each independent molecule of **1**, the coordinate bond distances are short, ranging between 1.856(8)-1.965(9) and 1.866(7)-1.956(8) Å, which points to a Co^{3+} oxidation state assignment. We have also synthesized a mononuclear complex **2**, which is a Co^{3+} complex of a structurally related but monotopic ligand HL^2 (Figure 1). In the molecular structure of $[CoL_2^2]ClO_4$ (**2**) (ESI†) the coordinate bond distances are similar to those observed in **1** (range = 1.859(4)-1.919(4) Å). Complex **2** is diamagnetic (ESI†) and contains Co^{3+}, which supports our assertion of Co^{3+} in **1**. In **1,** the lack of any counter-anions in the structure necessarily results in a charge of -3 for the ligand, which would render the ligand oxidation state in complex **1** a trianion-radical. Bond distances within the coordinated ligand vary considerably between the two metal ion binding pockets within the same ligand. In one pocket, the C-O and N-N bonds are considerably longer than those in the other pocket [C1-O6 = 1.306(11) and C24-O2 = 1.271(12) Å; N1-N2 = 1.305(11) and N5-N6 = 1.239(11) Å], while the C-N (bond joining the acyclic N atom to the terminal ring) bond is much shorter C6-N1 = 1.311(13) vs C19-N6 = 1.425(12) Å. Bond distances within the terminal rings range from 1.361(14)-1.459(14) Å (C1-to-C6) and 1.367(16)-1.459(14) Å (C19-to-C24).

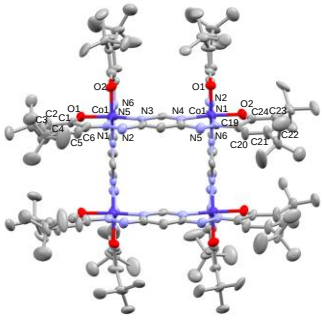

Figure 2. Molecular structure of **1** showing one of two molecules in the asymmetric unit (expanded ORTEP-style structure). Bond distances (Å) [with standard uncertainties (su) in brackets]: Co(1)-O(1), 1.901(6); Co(1)-O(2), 1.898(6); Co(1)-N(1), 1.856(8); Co(1)-N(3), 1.944(9); Co(1)-N(4), 1.965(9); Co(1)-N(6), 1.859(8); O(1)-C(1), 1.306(11); O(2)-C(24), 1.271(12); N(1)-N(2), 1.305(11); N(5)-N(6), 1.239(11).

The UV-VIS-NIR spectrum of complex **1** together with a model complex **2** is presented in Figure 3 (left). The spectrum of **1** is substantially different from typical metal arylazo ligand complexes, including other polynuclear [2×2] grid-type complexes reported earlier, which typically feature intense visible absorptions.[50] In the spectrum of **1**, broad and intense visible absorption bands are observed but also another very broad and low energy band is observed in the NIR (~1500 nm), which is not observed in the spectra of other arylazo complexes. We optimized the geometry of the trianion-radical (S = ½) state of the ligand (ESI†) and calculated the absorption spectrum of this species (ESI†) and a strong, broad band is calculated at 1554 nm, closely matching what is observed in complex **1** (Figure 3, left). This absorption is assigned to a α/HOMO-α/LUMO transition and is likely of similar character in **1**. We measured the temperature dependence of the UV-VIS-NIR absorption of **1** (between 373 to 200 K) and found no significant variation in the spectra (ESI†), which indicated a static electronic structure for **1** *in solution* over this temperature range. We have assessed the stability of **1** in solution by measuring the UV-visible and ESI mass spectra over time and found that while **1** is relatively stable in solution it does gradually oxidize (ESI†). The electrochemical properties of **1** (Figure 3, right) were measured by cyclic (ESI†) and differential pulse voltammetry and a large number of closely-spaced waves were observed over a large potential window. The low potential anodic processes can be assigned to oxidation of the ligand trianion-radicals and the cathodic processes represent $Co^{3+/2+}$ couples.

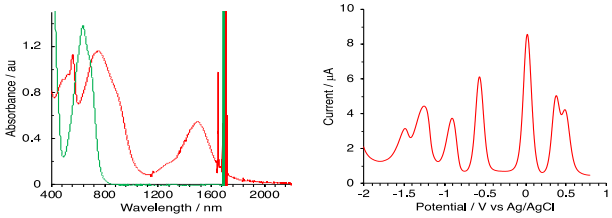

Figure 3. UV-VIS-NIR spectrum (left) of **1** (red trace) and **2** (green) in CH_2Cl_2. Differential pulse voltammogram (right) of **1** in CH_2Cl_2.

We used DFT calculations to support our hypothesis that the crystal of complex **1** solved at 100(2) K contains four Co^{3+} ions coordinated to four trianion-radical equivalents of the ligand. Using the coordinates from the crystal structure, we calculated the energy of complex **1** in the quintet state (S = 2, four unpaired electrons ferromagnetically coupled) and also carried out broken symmetry calculations on spin-flipped M_S = 0 states.[51–53] In both the quintet and the broken symmetry M_S = 0 states (Figure 4 & ESI†), almost all of the spin density resides on the ligands. The spin density is widely distributed over the ligand, with substantial spin densities residing on the donor azo N atoms. The quintet and broken symmetry M_S = 0 states are nearly degenerate, with the quintet state calculated to be thermally excited. This suggests that the four unpaired electrons are antiferro- and ferro-magnetically coupled for face-to-face and neighboring ligands in **1**, respectively; the calculated magnetic exchange coupling parameters are $J_{face\text{-}to\text{-}}$

J_{face} = -36.2 and $J_{neighboring}$ = +6.47 cm^{-1} (ESI†).[54] Although the calculated values are overestimated, the very low temperature behaviour observed in the magnetization versus temperature experiments (Figure 5, left) likely results from the antiferromagnetic coupling between the four coordinated radicals in **1.**

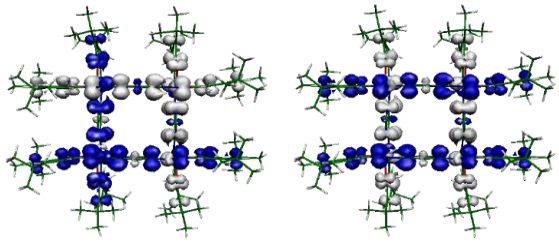

Figure 4. Spin densities (white is alpha spin density and blue is beta spin density) in the broken symmetry M_S = 0 states of complex **1** (BP86/def2-SVP). Left is M_S = 0 (BS, αααβ) and right is M_S = 0 (BS, αβαβ).

Variable temperature magnetic susceptibility measurements were carried out on pulverized single crystals of **1** from 2 K to 400 K (Figure 5, left). At 2 K, the value of $\chi_m T$ (1.43 cm^3 K mol^{-1}) is close to the expected value for four uncoupled organic radicals (4 × 0.375 = 1.5 cm^3 K mol^{-1}). With increasing temperature $\chi_m T$ values rise slightly (1.58 cm^3 K mol^{-1}) and then remain constant over the temperature range 6 – 45 K. Above 45 K, a significant increase in $\chi_m T$ is observed, with the values continuing their rise until approximately 370 K, where $\chi_m T$ is 2.49 cm^3 K mol^{-1} and remains so to 400 K. These data indicate that valence tautomerism is operative in **1**. With increasing temperature there is electron transfer from the ligand trianion-radical to Co^{3+}. The low value of $\chi_m T$ observed at 400 K suggests that only one electron is transferred between the four ligands and Co^{3+} ions (Scheme 1), which is likely distributed over the four cobalt ions. One localized high spin Co^{2+} ion and three S = ½ radicals would produce a $\chi_m T$ value close to what is observed at 400 K for **1**. No thermal hysteresis was noted from the magnetic susceptibility data but structural changes were indicated by the results of variable temperature EPR and FTIR.

$$[Co_4^{3+}L_4^{3\bullet-}] \rightleftarrows [(Co^{2+}L^{2-})(Co_3^{3+}L_3^{3\bullet-})]$$

Scheme 1. Description of the valence tautomerism equilibrium in the solid state of **1**.

Further support for VT in **1** was provided by EPR spectroscopy. Notable changes to the solid-state EPR spectrum (Figure 5, right & ESI†) of **1** with a change in temperature were observed. At 100 K, an intense signal centred at g = 2.00 was observed with no resolved hyperfine features. With warming to 400 K, the signal intensity was dramatically reduced, and additional transitions overlapping the broader absorption were observed. The low temperature spectrum can be assigned to spin multiplet states due to four weakly coupled organic radicals coordinated to the diamagnetic Co^{3+} ions; with warming the sample, the unpaired spin density transferred to cobalt, which was reduced to Co^{2+}. The electron transfer renders the transitions to which Co^{2+} contributes. The high-temperature spectrum takes time to slowly return back to the initial spectrum with decreasing temperature down to room temperature. The hysteresis behaviour associated with the electron transfer possibly accompanies a structural change. Variable temperature infrared spectroscopy experiments on **1** in the solid state confirm these structural changes that accompany the electron transfer (ESI†).

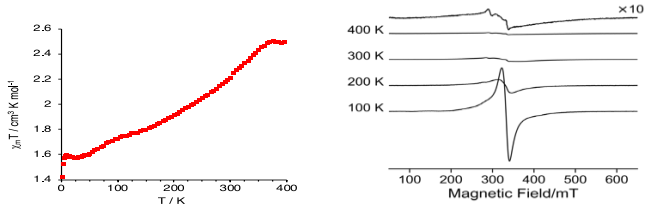

Figure 5. Variable temperature magnetic susceptibility data for **1** (left, 10 kOe field). Temperature dependence of the solid-state EPR spectra (right) of **1**.

In summary, we have reported a tetranuclear cobalt [2×2] grid valence tautomer. We are pursuing the coordination chemistry of this and related ditopic ligands with the goal of producing polynuclear VT multistate switching materials.

Financial support from NSERC (RGPIN 2015-05230 & 2015-06061 & CGS D), CFI, CRC and Brock University is acknowledged. This work was partially supported by KAKENHI Scientific Research B (17H03012 and 18H01955), Scientific Research C (18K03465), and Scientific Research S (19H05621) from the JSPS, Japan. This work was also supported by the AOARD Scientific Project on "Molecular Spins for Quantum Technologies" (FA2386-17-1-4040, 4041), U.S. Dr. P. Dube (McMaster) is acknowledged for acquiring magnetic susceptibility data.

Conflicts of interest

There are no conflicts to declare.

Notes and references

1 B. L. Feringa, *Angew. Chem. Int. Ed.*, 2017, **56**, 11060–11078.
2 Y. Wang, M. Frasconi and J. F. Stoddart, *ACS Cent. Sci.*, 2017, **3**, 927–935.
3 M. A. Halcrow, *Spin-Crossover Materials*, John Wiley & Sons Ltd, Oxford, UK, 2013.
4 D. J. Harding, P. Harding and W. Phonsri, *Coord. Chem. Rev.*, 2016, **313**, 38–61.
5 S. Hayami, K. Hiki, T. Kawahara, Y. Maeda, D. Urakami, K. Inoue, M. Ohama, S. Kawata and O. Sato, *Chem. Eur. J.*, 2009, **15**, 3497–3508.
6 N. Phukkaphan, D. L. Cruickshank, K. S. Murray, W. Phonsri, P. Harding and D. J. Harding, *Chem. Commun.*, 2017, **53**, 9801–9804.
7 D. Rosario-Amorin, P. Dechambenoit, A. Bentaleb, M. Rouzières, C. Mathonière and R. Clérac, *J. Am. Chem. Soc.*, 2018, **140**, 98–101.

8 B. Weber, W. Bauer and J. Obel, *Angew. Chem. Int. Ed.*, 2008, **47**, 10098–10101.
9 S. Hayami, Z. Gu, H. Yoshiki, a Fujishima and O. Sato, *J. Am. Chem. Soc.*, 2001, **123**, 11644–50.
10 T. Tezgerevska, K. G. Alley and C. Boskovic, *Coord. Chem. Rev.*, 2014, **268**, 23–40.
11 O. Drath and C. Boskovic, *Coord. Chem. Rev.*, 2017, **375**, 256–266.
12 R. M. Buchanan and C. G. Pierpont, *J. Am. Chem. Soc.*, 1980, **102**, 4951–4957.
13 D. M. Adams, L. Noodleman and D. N. Hendrickson, *Inorg. Chem.*, 1997, **36**, 3966–3984.
14 D. M. Adam, A. Dei, A. L. Rheingold and D. N. H. J, *J. Am. Chem. Soc.*, 1993, **1**, 8221–8229.
15 O.-S. Jung, D. H. Jo, Y.-A. Lee, B. J. Conklin and C. G. Pierpont, *Inorg. Chem.*, 1997, **36**, 19–24.
16 A. Dei, D. Gatteschi, C. Sangregorio and L. Sorace, *Acc. Chem. Res.*, 2004, **37**, 827–35.
17 E. Evangelio and D. Ruiz-Molina, *Eur. J. Inorg. Chem.*, 2005, **2005**, 2957–2971.
18 I. L. Fedushkin, O. V. Maslova, A. G. Morozov, S. Dechert, S. Demeshko and F. Meyer, *Angew. Chem. Int. Ed.*, 2012, **51**, 10584–10587.
19 I. Ratera, D. Ruiz-Molina, F. Renz, J. Ensling, K. Wurst, C. Rovira, P. Gütlich and J. Veciana, *J. Am. Chem. Soc.*, 2003, **125**, 1462–3.
20 G. D'Avino, L. Grisanti, J. Guasch, I. Ratera, J. Veciana and A. Painelli, *J. Am. Chem. Soc.*, 2008, **130**, 12064–12072.
21 A. Lannes, Y. Suffren, J. B. Tommasino, R. Chiriac, F. Toche, L. Khrouz, F. Molton, C. Duboc, I. Kieffer, J. L. Hazemann, C. Reber, A. Hauser and D. Luneau, *J. Am. Chem. Soc.*, 2016, **138**, 16493–16501.
22 C. Lecourt, Y. Izumi, L. Khrouz, F. Toche, R. Chiriac, N. Bélanger-Desmarais, C. Reber, O. Fabelo, K. Inoue, C. Desroches and D. Luneau, *Dalton Trans.*, 2020, **49**, 15646–15662.
23 C. Fleming, D. Chung, S. Ponce, D. J. R. Brook, J. Daros, R. Das, A. Ozarowski and S. A. Stoian, *Chem. Commun.*, 2020, **56**, 4400–4403.
24 A. Rajput, A. K. Sharma, S. K. Barman, D. Koley, M. Steinert and R. Mukherjee, *Inorg. Chem.*, 2014, **53**, 36–48.
25 O. Co, M. K. Mondal and C. Mukherjee, *Chem. Commun.*, 2016, **52**, 11995–11998.
26 S. Maity, S. Kundu, S. Bera, T. Weyhermüller and P. Ghosh, *Eur. J. Inorg. Chem.*, 2016, **2016**, 3680–3690.
27 J. Bendix and K. M. Clark, *Angew. Chem. Int. Ed.*, 2016, **55**, 2748–2752.
28 D. G. Lonnon, S. T. Lee and S. B. Colbran, *J. Am. Chem. Soc.*, 2007, **129**, 5800–1.
29 Y. Shimazaki, F. Tani, K. Fukui, Y. Naruta and O. Yamauchi, *J. Am. Chem. Soc.*, 2003, **125**, 10512–10513.
30 O. Rotthaus, F. Thomas, O. Jarjayes, C. Philouze, E. Saint-Aman and J.-L. Pierre, *Chem. Eur. J.*, 2006, **12**, 6953–6962.
31 O. Rotthaus, V. Labet, C. Philouze, O. Jarjayes and F. Thomas, *Eur. J. Inorg. Chem.*, 2008, **2008**, 4215–4224.
32 S. Wiesner, A. Wagner, E. Kaifer and H.-J. Himmel, *Chem. Eur. J.*, 2016, 10438–10445.
33 K. G. Alley, G. Poneti, J. B. Aitken, R. K. Hocking, B. Moubaraki, K. S. Murray, B. F. Abrahams, H. H. Harris, L. Sorace and C. Boskovic, *Inorg. Chem.*, 2012, **51**, 3944–3946.
34 J. Tao, H. Maruyama and O. Sato, *J. Am. Chem. Soc.*, 2006, **128**, 1790–1791.
35 S. Bin-Salamon, S. H. Brewer, E. C. Depperman, S. Franzen, J. W. Kampf, M. L. Kirk, R. K. Kumar, S. Lappi, K. Peariso, K. E. Preuss and D. a Shultz, *Inorg. Chem.*, 2006, **45**, 4461–4467.
36 N. G. R. Hearns, J. L. Korcok, M. M. Paquette and K. E. Preuss, *Inorg. Chem.*, 2006, **45**, 8817–8819.
37 A. Sieber, C. Boskovic, R. Bircher, O. Waldmann, S. T. Ochsenbein, G. Chaboussant, H. U. Güdel, N. Kirchner, J. van Slageren, W. Wernsdorfer, A. Neels, H. Stoeckli-Evans, S. Janssen, F. Juranyi and H. Mutka, *Inorg. Chem.*, 2005, **44**, 4315–4325.
38 K. G. Alley, G. Poneti, P. S. D. Robinson, A. Nafady, B. Moubaraki, J. B. Aitken, S. C. Drew, C. Ritchie, B. F. Abrahams, R. K. Hocking, K. S. Murray, A. M. Bond, H. H. Harris, L. Sorace and C. Boskovic, *J. Am. Chem. Soc.*, 2013, **135**, 8304–8323.
39 A. Madadi, M. Itazaki, R. W. Gable, B. Moubaraki, K. S. Murray and C. Boskovic, *Eur. J. Inorg. Chem.*, 2015, 4991–4995.
40 Y. Suenaga and C. G. Pierpont, *Inorg. Chem.*, 2005, **44**, 6183–6191.
41 C. Carbonera, A. Dei, J.-F. Létard, C. Sangregorio and L. Sorace, *Angew. Chem. Int. Ed.*, 2004, **43**, 3136–3138.
42 G. K. Gransbury, B. N. Livesay, J. T. Janetzki, M. A. Hay, R. W. Gable, M. P. Shores, A. Starikova and C. Boskovic, *J. Am. Chem. Soc.*, 2020, **142**, 10692–10704.
43 T. Glaser, M. Heidemeier, R. Fröhlich, P. Hildebrandt, E. Bothe and E. Bill, *Inorg. Chem.*, 2005, **44**, 5467–5482.
44 B. Li, X.-N. Wang, A. Kirchon, J.-S. Qin, J.-D. Pang, G.-L. Zhuang and H.-C. Zhou, *J. Am. Chem. Soc.*, 2018, **140**, 14581–14585.
45 S. Samanta, P. Ghosh and S. Goswami, *Dalton Trans.*, 2012, **41**, 2213-2226.
46 N. Van Damme, A. J. Lough, S. I. Gorelsky and M. T. Lemaire, *Inorg. Chem.*, 2013, **52**, 13021–13028.
47 N. Paul, S. Samanta and S. Goswami, *Inorg Chem*, 2010, **49**, 2649–2655.
48 N. D. Paul, U. Rana, S. Goswami, T. K. Mondal and S. Goswami, *J. Am. Chem. Soc.*, 2012, **134**, 6520–6523.
49 A. Sanyal, S. Chatterjee, A. Castiñeiras, B. Sarkar, P. Singh, J. Fiedler, S. Zális, W. Kaim and S. Goswami, *Inorg. Chem.*, 2007, **46**, 8584–8593.
50 N. M. Bonanno, N. Van Damme, A. J. Lough and M. T. Lemaire, *Dye. Pigment.*, 2015, **123**, 212–217.
51 A. P. Ginsberg, *J. Am. Chem. Soc.*, 1980, **102**, 111–117.
52 L. Noodleman, *J. Chem. Phys.*, 1981, **74**, 5737–5743.
53 L. Noodleman and E. R. Davidson, *Chem. Phys.*, 1986, **109**, 131–143.
54 T. Soda, Y. Kitagawa, T. Onishi, Y. Takano, Y. Shigeta, H. Nagao, Y. Yoshioka and K. Yamaguchi, *Chem. Phys. Lett.*, 2000, **319**, 223–230.